NORGES TEKNISK-NATURVITENSKAPELIGE
UNIVERSITET

Uncertainty in Production Forecasts based on Well Observations, Seismic Data and Production History

by

Bjørn Kåre Hegstad and Henning Omre

PREPRINT
STATISTICS NO. 17/1999

NORWEGIAN UNIVERSITY OF SCIENCE AND
TECHNOLOGY
TRONDHEIM, NORWAY

This report has URL http://www.math.ntnu.no/preprint/statistics/1999/S17-1999.ps
Henning Omre has homepage: http://www.math.ntnu.no/~omre
E-mail: omre@stat.ntnu.no
Address: Department of Mathematical Sciences, Norwegian University of Science and Technology,
N-7491 Trondheim, Norway.

Uncertainty in Production Forecasts based on Well Observations, Seismic Data and Production History

Bjørn Kåre Hegstad and Henning Omre
Department of Mathematical Sciences
Norwegian University of Science and Technology
Trondheim, Norway

May 1999

Abstract

A stochastic model in a Bayesian setting, conditioned on well observations, seismic amplitude data and production history is defined on a graph. Samples of reservoir characteristics and production forecasts from the posterior model are used to evaluate the impact of various observation types. Well observations are found to be important to production forecasts due to near-well conditioning, seismic data impact facies geometries but not strongly the production forecasts. Jointly, the well and seismic data provide reliable samples of reservoir characteristics and general production forecasts. Production history do only contribute significantly if certain events like gas-break-through time is observed in wells. A brute force rejection sampling approach may work well if proper conditioning on well observations and seismic data is done.

1 Introduction

The objective of reservoir evaluation is to forecast production characteristics under various recovery strategies, and eventually decide on a management strategy. The forecasts should be as accurate and precise as possible, hence both general reservoir knowledge and reservoir specific observations should be used in the evaluation. General reservoir knowledge include geologic understanding, physically based models for fluid flow and insight into the data acquisition procedures. The reservoir specific observations include well observations, seismic amplitude data and production history collected from the reservoir under study. In Omre and Tjelmeland (1997) a Bayesian approach to integrated reservoir evaluation is presented.

Stochastic reservoir modeling based on geologic knowledge and well observations only, has taken place in two decades. Inclusion of seismic amplitude data has been an active field of research the last years, see Bortoli et al. (1993) and Eide et al. (1999). In order to represent the uncertainty, seismic inversion must be a part of the model. History matching of production data has only recently been phrased in a stochastic setting, see Oliver (1994), Wen et al. (1997) and Hegstad and Omre (1997). This requires the use of a fluid flow simulator which normally needs considerable computer resources to run.

The current paper integrates all these sources of information in a framework defined along the lines of Omre and Tjelmeland (1997). A graphical model is introduced to communicate the model assumptions more easily to the user. Models and algorithms developed in Eide et al. (1999) and Hegstad and Omre (1997) are integrated and applied to a case study inspired by the Troll Field in the North Sea. The focus of the paper is to evaluate the contribution of the well observations, seismic amplitude data and production history, respectively, to the reduction of uncertainty in the production forecasts. Conditioning to the production history constitutes a major challenge due to the non-linearity of the fluid flow model. The study also throw some light on which sampling algorithms being suitable for this. The study is thoroughly documented in Hegstad and Omre (1998) in which further details can be found.

2 Reference reservoir and production

The reference reservoir and the recovery strategy are inspired by the Troll field in the North Sea offshore Norway, see Eide et al. (1999). It is a multi-layer reservoir with alternating C-sands and M-sands having high and low permeability properties respectively. The reservoir is represented in a three-dimensional domain $[(x_1, x_2), y] \in \mathcal{D}_x \times \mathcal{D}_y \subset \mathcal{R}^2 \times \mathcal{R}$ being $[10^4 \times 10^4 \times 10^2]$ feet^3, being discretized into a $(50 \times 50 \times 15)$-grid termed $\mathcal{L}_\mathcal{D}$. The primary interest of the study is future production being crucially dependent on the reservoir variables: porosity and absolute log-permeability. The acoustic impedances and seismic reflection coefficients are introduced as support variables. These spatial reservoir variables are defined as a high-dimensional vector on the grid $\mathcal{L}_\mathcal{D}$ by $(r^t_\phi, r^t_k, r^t_z, r^t_c)$ with indexes (ϕ, k, z, c) indicating porosity, absolute log-permeability, acoustic impedance and seismic reflection coefficients respectively; and index t indicating that it is the reference reservoir. The lateral-vertical anisotropy in permeability is $1 : 600$. A more detailed description of the construction can be found in Hegstad and Omre (1998). The cross section of the reference reservoir, displayed in Figure 1, shows distinct layering. The histograms and cross plots of the reservoir variables, in Figure 2, display definite bi-modality and clustering. The reference reservoir variables have characteristics far from Gaussian. The initial saturation is assigned oil everywhere and the reservoir is in pressure equilibrium at production start. For further details and other fluid characteristics see Hegstad and Omre (1998).

The recovery strategy is based on injection of gas in one vertical well perforated in the upper layers, and production through two horizontal wells, see Figure 3. The reference production is generated by the fluid flow simulator Eclipse100, see GeoQuest (1997), on a $(10 \times 10 \times 15)$ laterally upscaled grid. The permeability characteristics are upscaled by harmonic averaging while the other variables are upscaled by arithmetic averaging. For further details see Hegstad and Omre (1998). The oil-production-rate and gas-oil-ratio in the two producing wells and the bottom-hole-pressure in the injection well are monitored monthly for 16 years, i.e. 5840 days. This is represented by the time vector $(p^t_{\text{opr}}, p^t_{\text{gor}}, p^t_{\text{bhp}})$, on $\mathcal{L}_\mathcal{T}$, see Figure 4. Note that gas-break-through appears after about 3 years, and that the plateau production is defended in about 5 years.

3 Stochastic model and simulation algorithm

The stochastic model consists of two components: a prior model for the reservoir and production variables, and a likelihood function model for the reservoir specific observations available. The stochastic model is graphically displayed in Figure 5.

The stochastic reservoir variables are termed $R = (R_\phi, R_k, R_z, R_c)$ defined on $\mathcal{L}_\mathcal{D} : (50 \times 50 \times 15)$ and the stochastic production variables are termed $P = (P_{\text{opr}}, P_{\text{gor}}, P_{\text{bhp}})$ defined over $\mathcal{L}_\mathcal{T}$, i.e. monthly for 16 years. The reservoir specific observations appear from wells, d_w, consisting of observations of the reservoir variables along the well traces $(r^o_\phi, r^o_k, r^o_z, r^o_c)$; seismic data, d_s, being seismic amplitude data on $\mathcal{L}_\mathcal{D}$, s^o_a, and production data, d_p, consisting of production history the first 4.5 years, $p^o_q = (p^o_{\text{opr}}, t^o_{\text{gor}}, p^o_{\text{bhp}})$, with q indicating dependence on the recovery strategy q and t^o_{gor} being the time for gas-break-through, if observed.

4 Prior model

The prior model of the reservoir and production variables must be based on general understanding of the reservoir and fluid flow processes.

The porosity given impedance is modeled as:

$$[R_\phi | r_z] = \mu_\phi(r_z) + U_\phi \tag{1}$$

with $\mu_\phi(r_z)$ being a location-wise, linear function, $a + br_z$; and U_ϕ being a discretized, Gaussian random field with zero expectation and covariance matrix Σ_ϕ determined by the spatial covariance function $\sigma^2_\phi \rho(\cdot\,; \nu_\phi)$ defined by the exponential correlation function:

$$\rho(\Delta; \nu) = \exp\{-3\|\Delta'\|^\nu\} \tag{2}$$

with $\Delta' = [\Delta_{x_1}/20000, \Delta_{x_2}/20000, \Delta_z/33.3]$. Hence the porosity is linearly related to acoustic impedance in the corresponding location plus a residual Gaussian random field. The parameter values actually used are presented in Table 1, and they are obtained from Eide (1997) and discussions with geoscientists. This defines the conditional pdf $f(r_\phi | r_z)$ to be Gaussian and it is denoted by the single arrow from R_z to R_ϕ on Figure 5.

The absolute log-permeability given acoustic impedance and a parameter vector $\theta = (\theta_1, \theta_2)$ is:

$$[R_k | r_z, \theta] = \mu_k(r_z; \theta) + U_k(r_z) \tag{3}$$

with

$$\mu_k(r_z; \theta) = \begin{cases} \theta_1 & \text{if } r_z \geq t_z \\ \theta_2 & \text{else} \end{cases} \tag{4}$$

being a location-wise step-function defined by the threshold t_z and the stochastically defined levels $\Theta = (\Theta_1, \Theta_2)$, being Gaussian with expectation μ_θ and diagonal covariance matrix Σ_θ. The $U_k(r_z)$ is a discretized Gaussian random function with zero expectation and covariance matrix Σ_k determined from the spatial covariance function $\sigma^2_k(r_z)\rho(\cdot\,; \nu_k)$ with

$$\sigma^2_k(r_k) = \begin{cases} \sigma^2_{k,1} & \text{if } r_z \geq t_z \\ \sigma^2_{k,2} & \text{else} \end{cases} \tag{5}$$

and $\rho(\cdot;\nu)$ being an exponential correlation function as previously defined. The lateral-vertical anisotropy factor is $1:600$. Hence the log-permeability is related to a facies concept defined by a cut-off, t_z, and acoustic impedance. The permeability level in each facies, $\Theta = (\Theta_1, \Theta_2)$, is stochastically defined, and the heterogeneity in each facies varies, $(\sigma^2_{k,1}, \sigma^2_{k,2})$. Moreover, the porosity and log-permeability are only related through this facies concept being defined by the acoustic impedance. This is according to the findings in Troll data. The parameter values actually used are listed in Table 1. This defines the conditional pdf $f(r_k|r_z,\theta)$ to be Gaussian, represented by arrows from R_z and Θ to R_k in Figure 5. The log-permeability levels are assigned a Gaussian prior model, $f(\theta)$, with expectation μ_θ and diagonal covariance matrix Σ_θ, and actual parameter values listed in Table 1. Consequently $f(r_k,\theta|r_z)$ is Gaussian also.

The seismic reflection coefficients are defined through the acoustic impedance by $R_c(x,y) = \frac{1}{2}\frac{d}{dy}\ln R_z(x,y)$, see Sheriff and Gelhart (1982), which discretizes into

$$R_c(x,y_i) = \frac{R_z(x,y_{i+1}) - R_z(x,y_i)}{R_z(x,y_{i+1}) + R_z(x,y_i)} \tag{6}$$

and inversely, the recursion:

$$R_z(x,y_{i+1}) = \frac{1 + R_c(x,y_i)}{1 - R_c(x,y_i)} R_z(x,y_i) \tag{7}$$

with $y_i; i = 1, \dots, 15$ being the vertical discretization. Hence given $R_{z,\text{top}} = r_{z,\text{top}} = \{r_z(x,y_1); x \in \mathcal{D}_x\}$, i.e. the acoustic impedance on the top of the reservoir, there is a non-linear one-to-one relation between the two. This defines the conditional pdf $f(r_z|r_c)$ as a Dirac pdf, with the dependence on $r_{z,\text{top}}$ suppressed in the notation. This relation is represented by a double arrow from R_c to R_z in Figure 5.

The procedure for obtaining the $r_{z,\text{top}}$ is specified in Hegstad and Omre (1998), and the problem is further complicated by $r_{z,\text{top}}$ being required to reproduce the observations. This problem has not found its final solution and should be subject to further research.

The prior model assigned to the seismic reflection coefficients is a discretized, Gaussian random function with expectation zero and covariance matrix Σ_c. The latter is defined from the spatial covariance function $\sigma_c^2\rho_c(\cdot\,;\nu_c)$. The correlation function being a discretized version of:

$$\rho((\Delta_x,\Delta_y);\nu) = -\frac{\partial^2}{\partial^2\Delta_y}[\rho((\Delta_x,\Delta_y);\nu)] \tag{8}$$

with $\rho(\cdot\,;\nu)$ being the exponential correlation function previously defined. This is justified by the reflection coefficients being related to the derivative of acoustic impedance being slowly varying in space. This model entails that reflection coefficients appears with pseudo-periodicity vertically which is according to empirical studies, see Todoenschunck and Jensen (1988). The parameter values actually used are obtained from Eide (1997). This defines the prior pdf $f(r_c)$ to be Gaussian.

It is also assumed that the initial reservoir conditions are known, i.e. it contains oil only and that it is in pressure equilibrium. The other less important reservoir variables can be found in Hegstad and Omre (1998).

This completes the definition of the prior stochastic model for the reservoir variables. The most important ones are contained in $R = (R_\phi, R_k, R_z, R_c)$, and graphically displayed in Figure 5. Note that each of them are defined on the grid $\mathcal{L}_\mathcal{D}$ covering the reservoir. The prior pdf for this is:

$$\begin{aligned} f(r,\theta) &= f(r_\phi, r_k, r_z, r_c, \theta) \\ &= f(r_\phi|r_z) f(r_k|r_z,\theta) f(r_z|r_c) f(r_c) f(\theta) \end{aligned}$$

which can be seen from the conditional independencies implicitly defined in the graph in Figure 5. This factorization into conditional Gaussian or Dirac factors does also provide an efficient sequential algorithm for sampling from the prior pdf. Note that the prior pdf $f(r,\theta)$ will not be Gaussian since several conditioning variables are involved non-linearly in the factorization. The fact that θ is involved in the expression creates no problems in the sampling, since sampling (r,θ) and only retaining r will provide samples from $f(r)$. In Figure 6 cross sections of a representative sample from the prior pdf $f(r)$ are displayed. It is worth noting that the prior contains no information about the layering as such, only fairly strong lateral anisotropy, and hence geometries like in the reference reservoir, see Figure 1, have extremely low probability to occur. In that respect, this study can be considered as realistic.

The production variables $P = (P_{\text{opr}}, P_{\text{gor}}, P_{\text{bhp}})$ on the time grid $\mathcal{L}_\mathcal{T}$, are linked to the reservoir variables through the fluid flow simulator. The relation is as follows:

$$[P_q|r] = v(r;q) = v((r_\phi, r_k);q) \tag{9}$$

with $v(\cdot;q)$ being the fluid flow simulator with recovery strategy q including necessary upscaling of reservoir variables; and with the dependence on other reservoir variables like saturations and pressure which are assumed known, being suppressed in the notation. In this study the fluid flow simulator Eclipse100, see GeoQuest (1997), is used, and lateral upscaling to a $(10 \times 10 \times 15)$-grid is done by harmonic averaging of permeability properties and arithmetic averaging otherwise. The recovery strategy, q, is outlined in the previous section, and a complete definition can be found in Hegstad and Omre (1998). This defines the conditional pdf $f(p_q|r_\phi, r_k)$ as a Dirac pdf, being represented by double arrows in Figure 5.

The joint prior pdf of reservoir and production variables are:

$$f(p_q, r, \theta) = f(p_q|r) f(r,\theta) \tag{10}$$

and samples of p_q can be provided by using the fluid flow simulator on samples form the prior model provided above, see Figure 7. Note that the variability in the prior model is so large that in many cases the fluid flow simulator produces unphysical results. Hence little prior information is introduced through the prior pdf.

5 The likelihood model

The likelihood model must be based on understanding of the respective data acquisition procedures.

The well observations consist of porosity, absolute log-permeability, acoustic impedance and reflection coefficients data, $d_w = (r_\phi^o, r_k^o, r_z^o, r_c^o)$, along the well traces. Some of these observations are displayed in Figure 8. The corresponding likelihood models are:

$$\begin{aligned}
[R_\phi^o|r_\phi] &= A_w \cdot r_\phi \\
[R_k^o|r_k] &= A_w \cdot r_k \\
[R_z^o|r_z] &= A_w \cdot r_z \\
[R_c^o|r_c] &= A_w \cdot r_c
\end{aligned}$$

with A_w being a design matrix identifying the location of the well traces in the discretely represented reservoir domain. This entails that all well observations are assumed to be made without averaging or observation error. Note that this entails that the reflection coefficients must be consistent with the impedance due to their deterministic relation.

This defines the likelihood models $f(r_\phi^o|r_\phi)$, $f(r_k^o|r_k)$, $f(r_z^o|r_z)$ and $f(r_c^o|r_c)$, all being Dirac pdfs, represented by double arrows in Figure 5.

The seismic data consists of seismic amplitude observations in every node of the reservoir representation, constituting the vector $d_s = s_a^o$. A cross section of these data is presented in Figure 9. Note that seismic data originally are collected with a vertical time reference, these have however been depth converted in a preprocess. The likelihood model for the seismic data is:

$$[S_a^o|c] = A_s \cdot c + U_{s^o} \tag{11}$$

with A_s being a matrix defined by a Ricker wavelet with parameter 40 Hz; and U_{s^o} being a vector of independent Gaussian observation errors with zero expectation and variance $\sigma_s^2 = 0.15^2$. This corresponds to a seismic convolution model, see Sheriff and Gelhart (1982). Hence the seismic data are linearly related to the reflection coefficients, but non-linearly related to the reservoir variables of primary interest, namely porosity and permeability. This completes the definition of the likelihood model $f(s_a^o|c)$ being Gaussian and represented by a single arrow in Figure 5.

The production history contains observations of oil-production-rate and gas-oil-ratio in producing wells and bottom-hole-pressure in injection well for the first 4.5 years, i.e. 1642 days, see Figure 10. Note that this is after gas-break-through but prior to the production leaving the plateau rate. The observations are reduced to oil-production-rate and bottom-hole-pressure at days $(31, 821, 1642)$ and time of gas-break-through, $d_p = p_q^o = (p_{\mathrm{opr}}^o, t_{\mathrm{gor}}^o, p_{\mathrm{bhp}}^o)$. The likelihood models are:

$$\begin{aligned}
[P_{\mathrm{opr}}^o|p_{\mathrm{opr}}] &= A_h \cdot p_{\mathrm{opr}} + U_{P_{\mathrm{opr}}^o} \\
[T_{\mathrm{gor}}^o|p_{\mathrm{gor}}] &= \min\{t; p_{\mathrm{gor}} > \epsilon\} + U_{T_{\mathrm{gor}}^o} \\
[P_{\mathrm{bhp}}^o|p_{\mathrm{bhp}}] &= A_h \cdot p_{\mathrm{bhp}} + U_{P_{\mathrm{bhp}}^o}
\end{aligned}$$

with A_h being a design matrix identifying the days being observed; ϵ being a threshold; and $U_.$ being vectors of independent Gaussian model and observation errors with zero expectation and variance $\sigma_.^2$. The censoring in the observations at 4.5 years is solved by assigning a probability to time for gas-break-through as if it had been observed immediately after 4.5 years. This is a conservative choice, and the problem of censoring should be subject to further research.

In this study $\epsilon = 1.28$, $\sigma^2_{p^o_{\text{opr}}}$ and $\sigma^2_{p^o_{\text{bhp}}}$ are set to $(2.5\%)^2$ of observed value and $\sigma^2_{T^o_{\text{gor}}}$ set to $(50 \text{ days})^2$. This entails that the oil-production-rate and bottom-hole-pressure are observed with a precision of $\pm 5\%$ of the true value, while the break through time of gas is observed with precision ± 100 days. This completes the definition of the likelihood model, $f(p^o_q|p_q)$ being Gaussian, indicated by a single arrow in Figure 5.

By assuming independence between the observation error in the various data acquisition procedures, one can write $d = (d_s, d_w, d_p)$

$$f(d|r) = f(d_s|r)f(d_w|r)f(d_p|r) \tag{12}$$

in which the likelihood definitions previously defined can be inserted.

6 Model characteristics and sampling algorithms

Recall that all conditional prior pdfs indicated by single arrows in Figure 5, are Gaussian. All double arrows represent Dirac pdfs, or deterministic relations, which may be thought of as limiting Gaussian pdfs with the variances approaching zero. Moreover the prior models on reflection coefficients and log-permeability facies levels are Gaussian. This does not make the joint distribution of all the variables involved Gaussian, however. In the conditional pdfs, there appear several non-linear functions of the conditioning values. Examples are: facies cut-offs in acoustic impedance, non-linearity between acoustic impedance and reflection coefficients, indicator functions for observing gas break through time and not to mention the crucial non-linearity in the fluid flow simulator linking reservoir variables and production variables. All these functions of the conditioning values had to be linear to ensure Gaussianity in the joint pdf. Hence the stochastic model will not be subject to analytical evaluation, and one has to rely on sampling based techniques.

Forecasts of production is the primary objective of the study, but better representation of the reservoir variables will contribute to more efficient reservoir management. The posterior model of interest is:

$$f(p_q, r, \theta|d_s, d_w, d_p) = \text{const} \cdot f(d_p|p_q)f(p_q|r)f(r, \theta|d_s, d_w). \tag{13}$$

with "const" being a normalizing constant. The factorization is justified by the conditional independencies defined in the graph of Figure 5. Various sampling algorithms may be used to sample from this posterior pdf, see Omre et al. (1999). In this study a rejection sampling algorithm along the lines of Hegstad and Omre (1997) is used. It consists of proposing (p'_q, r') from $f(p_q|r)f(r, \theta|d_s, d_w)$ and then accepting it dependent on the value of $f(d_p|p'_q)$. The crucial factor in the algorithm is the acceptance rate since providing a proposal is very computer resource requiring due to the need for running the fluid flow simulator to obtain $f(p_q|r)$. The conditioning on both well and seismic data in the proposals will hopefully reduce the variability in the proposals such that a reasonable acceptance rate is obtained.

Sampling from the conditional pdf $f(r, \theta|d_w, d_s)$, required to provide a proposal, is not trivial either. An efficient algorithm for this is defined in Eide et al. (1999). The reliability of the algorithm depends on acoustic impedance and reflection coefficients being exactly observed whenever porosity and permeability data are available, and that the relations between porosity and permeability, and acoustic impedance, are local. The sampling algorithm is sequential and based on the following factorization:

$$
\begin{aligned}
f(r,\theta|d_w,d_s) &= f(r_\phi,r_k,r_z,r_c,\theta|r_\phi^o,r_k^o,r_z^o,r_c^o,s_a^o) \\
&= f(r_\phi|r_z,r_\phi^o)f(r_k|r_z,\theta,r_k^o)f(\theta|r_z,r_k^o)f(r_z|r_c)f(r_c|r_c^o,s_a^o)
\end{aligned}
$$

Note that all conditional pdfs on the right hand side are either Gaussian or Dirac pdfs, hence analytical evaluation and familiar sampling algorithms can be used. The term $f(r_c|r_c^o,s_a^o)$ is somewhat complicated due to high dimensionality of the conditioning seismic data, but a solution along lines of Eide et al. (1999), further discussed in Hegstad and Omre (1998), is chosen.

7 Results and discussion

Forecasts of production and prediction of reservoir variables with uncertainty assessments are defined by the posterior pdf $f(p_q,r,\theta|d_w,d_s,d_p)$. Samples of (p_q,r) from this pdf will represent the uncertainty. In this section some results of the study will be presented. Additional results can be found in Hegstad and Omre (1998).

The ultimate objective is to forecast production beyond the 4.5 years observed, and to assess the uncertainty in these forecasts. Figure 11 contains samples of $f(p_q|d_w,d_s,d_p)$, overlayed the reference production. All samples reproduce the conditioning on (d_w,d_s,d_p) up to the precision in the likelihood model. Recall that the prior model is relatively wide, see Figure 6, hence almost all constraints come from the reservoir specific observations. Note in particular that the gas break through time is reproduced as in d_p, but that the time for plateau rate decline is more variable since it is not observed at time 4.5 years. The samples are reasonably well centered at the reference production although some difference in general shape can be observed in well 1. This is probably due to the reference reservoir being extreme relative to the prior model. The uncertainty in forecasts of oil-production-rate is largest just after it has left the plateau, not in the distant future. This makes sense since the time for leaving the plateau may be crucially dependent on relatively small scale heterogeneities in the reservoir while the limiting rate is primary dependent on large scale, average properties. The small scale features are harder to predict hence leaving larger uncertainty.

It is important to note that the production forecasts above are based on a recovery strategy involving only the existing wells. If new, non-observed, infill wells are included, the uncertainty may increase dramatically. Moreover, the results will in this case be crucially dependent on the ability to predict the reservoir variables, with less impact of the production history.

In the following paragraphs the dependencies on the various pieces of reservoir specific observations $d=(d_w,d_s,d_p)$ will be evaluated. In order to make the comparison easier, the level of permeability in each facies is assumed known, i.e. $\theta=\theta^t$, being equal to the level used in the reference reservoir, see Table 1. Consider the case with only well observations, d_w, available. The posterior pdf of interest is $f(p_q,r|d_w,\theta^t)$, and samples of production forecasts are presented in Figure 12 and a cross section of a representative sample of the reservoir variables are presented in Figure 13. By comparing the production forecasts with the best forecasts in Figure 11, one observes that the general pattern is reasonable well reproduced although with considerably less precision. The times for gas-break-through and plateau rate decline are highly variable. The sample of the reservoir variables is very different from the reference reservoir in Figure 1. The general facies geometry is not very well reproduced. The reason for production forecasts to be reliable while the reservoir variables are relatively poorly reproduced comes from the fact that fluid flow is primary determined by the reservoir properties close to the wells, which are reliably characterized by the well observations.

Consider the case with only seismic data, d_s, available. The posterior pdf of interest is $f(p_q, r|d_s, \theta^t)$, and samples of production forecasts are presented in Figure 14 and a representative sample of reservoir variables in Figure 15. Note that the reservoir variables are remarkably similar to the reference reservoir, see Figure 1. The reason for the production forecast to be so poor is probably the great uncertainty in the value of the reservoir variables in the vicinity of the wells.

Consider the case with both well and seismic observations, d_w and d_s, but no production history, d_p. The posterior pdf of interest is $f(p_q, r|d_w, d_s, \theta^t)$ with results displayed in Figure 16 and Figure 17. The production forecasts are slightly improved relative to the ones based on well observations only, see Figure 12, and the reservoir variables are slightly improved relative to the ones based on seismics only, see Figure 15. One gets the best from both worlds, of course. The real advantage of conditioning on both well and seismic data comes when evaluation of various infill drill programs are needed.

In Figure 11, production forecasts from the posterior $f(p_q, r|d_w, d_s, d_p)$ hence conditioned on both well observations, seismic data and production history up to 4.5 years, are displayed. The corresponding reservoir variable samples are very similar to the ones based on well and seismic data only, see Figure 17, and hence not presented. Consider now the production forecast based on d_w, d_s and d_p^* with the latter being production history up to 2.5 years, i.e. hence prior to gas-break-through. The results are displayed in Figure 18. Note that the variability is much larger than in Figure 11, and this is particularly true for gas-break-through time and time for decline from the plateau rate. The forecasts are indeed comparable to the ones based on well observations and seismic data only, without production history at all, see Figure 16. Hence production history data seem to carry very little information before gas-break-through is observed.

The comparison above is not completely fair, since forecasts based on d_w and d_s are also conditioned on $\theta = \theta^t$ which the history matched forecasts are not. Consider therefore the posterior pdfs of the levels of the permeability in the two facies, Θ. From Figure 19 it can be seen that well observations and seismic data significantly improve the prediction of Θ, while the production data only have marginal influence. This may be surprising since the production is believed to be very dependent on the permeability level.

Recall that in the prior model no explicit information about the layering is included. A strong lateral anisotropy, exponential correlation function with range twice the reservoir extent, is assumed, however. Assume now that a prior model with lateral range 10^4 feet, hence the extent of the reservoir, and vertical range 20 feet is used. This will of course reduce the spatial influence of the well observations. In Figure 20 and Figure 21 the production forecasts based on $f^u(p_q, r|d_w, \theta^t)$ and $f^u(p_q, r|d_w, d_s, \theta^t)$ respectively, under this prior model are presented. The uncertainty increases dramatically for forecasts based on well observations, d_w, only relative to the forecasts based on the other prior model, see Figure 16. The bias in the forecast is alarming. Including the seismic data, d_s, cause a significant improvement in the forecasts, however, and their uncertainty is comparable to the forecasts under the other prior model, see Figure 16.

The computer resources required for history matching in a stochastic setting are crucial. In the algorithm used here, the acceptance rate in the rejection sampling step is the critical factor. When sampling from $f(p_q, r|d_p)$, hence conditioning on production history only, the acceptance rate is virtually zero. This is caused by the probability of sampling reservoir variables from the prior $f(r)$ close to the reference reservoir being extremely low. The same is true for $f(p_q, r|d_s, d_p)$, hence conditioning on seismic data and production history, since the actual level of the reservoir variables is largely unknown. Sampling from $f(p_q, r|d_w, d_p)$, hence conditioning on well observations and production history is feasible, however, with acceptance rate about 1.5%. By also including seismic data, and hence sample form $f(p_q, r|d_w, d_s, d_p)$, the acceptance rate is doubled to 3.0%. The need for in average only 33 fluid flow simulations in order to obtain one sample make the rejection algorithm close to feasible in real studies. If the production history for only 2.5 years is available, hence sampling from $f(p_q, r|d_w, d_s, d_p^*)$, the acceptance rate increases dramatically to 88.0%. Approximate algorithms based on optimization, see Omre et al. (1999) and Gómez-Hernández et al. (1997), which require additional costs for sensitivity computation, is not expected to do significantly better than this. Moreover, the rejection algorithm provides correct samples while the approximations from the other algorithms in many cases can be poor.

8 Conclusion

Assessing uncertainties in production forecasts conditioned on both well observations, seismic amplitude data and production history, is a hard problem. It is important to explicitly state the model assumptions, hence defining with respect to which model the uncertainty statements are made. Phrasing the model in a Bayesian setting using a graph to communicate it, appears as useful. Note further that many of the assumptions in the current study can be relaxed without making the computational burden larger. Examples are non-linear dependencies of conditioning variables and error terms in the likelihood models.

The reference reservoir is inspired by the Troll Field in the North Sea. The prior model is chosen such that the probability of the reference reservoir is extremely small. Hence the production forecasts rely crucially on the reservoir specific observations. The results of the study can be summarized by:

- Well observations contain little information about facies geometries. Strong lateral correlation in the prior model makes the well observations reproduce the production reasonably close, but the uncertainty in the forecasts increase fast with decreasing lateral correlation.

- Seismic amplitude data help reproducing the facies geometries. These data have limited impact on the production forecasts, however, since near-well regions and absolute values of the reservoir characteristics are poorly defined by the seismic data.

- Well observations and seismic amplitudes together, provides fairly reliable samples of reservoir variables and forecasts of production. Although forecasts of specific characteristics like gas-break-through times for individual wells are associated with large uncertainty.

- Production history does only reduce uncertainty significantly when it includes information about specific events like for example gas-break-through time in individual wells.

The study is based on production forecasts from the same well configuration as the reservoir is conditioned on. If additional, non-observed, infill wells are included, the uncertainty in the forecasts are expected to increase substantially. The impact of the uncertainty in prediction of reservoir variables will then increase.

The efficiency of the sampling algorithm is crucially dependent on the number of fluid flow simulator runs needed in order to obtain one sample. In the rejection sampling algorithm used here, on average one in 33 samples is accepted. This may indicate that a brute force approach as rejection sampling, is feasible when proper conditioning on both well observations and seismic amplitude data is done.

9 Acknowledgment

The work was financed through a post doc. grant from Norsk Hydro asa. Eivind Damsleth, Charlotte Tjølsen and other Norsk Hydro personnel contributed in defining the reference reservoir. Alfhild Lien Eide and Håkon Tjelmeland provided the base-code for seismic inversion.

References

Bortoli, L.-J., F. Alabert, A. Haas, and A. Journel (1993). Constraining stochastic images to seismic data: Stochastic simulation of synthetic seismograms. In A. Soares (Ed.), *Geostatistics Tróia '92*, pp. 325–337. Kluwer Academic Publishers. Proceedings from the Fourth International Geostatistical Congress, Tróia, Portugal, September 1992.

Eide, A. L. (1997). Stochastic simulation of porosity and acoustic impedance conditioned to seismic data and well data from the Troll field. Technical Report Statistics 12/1997, Norwegian University of Science and Technology. http://www.math.ntnu.no/preprint.

Eide, A. L., H. Omre, and B. Ursin (1999). Uncertainty in seismic inversion for reservoir characterization. Technical Report Statistics 10/1999, Norwegian University of Science and Technology. http://www.math.ntnu.no/preprint.

GeoQuest (1997). Eclipse 100, reference manual. GeoQuest Reservoir Technologies, Schlumberger.

Gómez-Hernández, J. J., J. E. Capilla, and A. Sahuquillo (1997). Inverse conditional simulation. In E. Y. Baafi and N. A. Schofield (Eds.), *Geostatistics Wollongong'96*, Volume I, pp. 282–291. Kluwer Academic Publishers. Proceedings from the Fifth International Geostatistical Congress, Wollongong, Australia, 22.-27. September 1996.

Hegstad, B. K. and H. Omre (1997). Uncertainty Assessment in History Matching and Forecasting. In E. Y. Baafi and N. A. Schofield (Eds.), *Geostatistics Wollongong'96*, Volume I, pp. 585–596. Kluwer Academic Publisher. Proceedings from the Fifth International Geostatistical Congress, Wollongong, Australia, 22.-27. September 1996.

Hegstad, B. K. and H. Omre (1998). Reservoir characterization integrating well observations, seismic data and production history. Technical Report Statistics 11/1998, Norwegian University of Science and Technology. http://www.math.ntnu.no/preprint.

Oliver, D. S. (1994). Multiple Realizations of the Permeability Field From Well Test Data. *University of Tulsa Centennial Petroleum Engineering Symposium*, pp. 145–153. Tulsa, Oklahoma, USA, August 29-31, 1994. SPE 27970.

Omre, H. and H. Tjelmeland (1997). Petroleum geostatistics. In E. Y. Baafi and N. A. Schofield (Eds.), *Geostatistics Wollongong'96*, Volume I, pp. 41–52. Kluwer Academic Publishers. Proceedings from the Fifth International Geostatistical Congress, Wollongong, Australia, 22.-27. September 1996.

Omre, H., H. Tjelmeland, and H. T. Wist (1999). Uncertainty in history matching - model specification and sampling algorithms. Technical Report Statistics 6/1999, Norwegian Univeristy of Science and Technolgy. http://www.math.ntnu.no/preprint.

Sheriff, R. E. and L. P. Gelhart (1982). *Exploration Seismology. History, theory and data aquisition.* Cambridge University Press.

Todoenschunck, J. P. and O. G. Jensen (1988). Joseph geology and seismic deconvolution. *Geophysics 53*(11).

Wen, X., C. V. Deutsch, and A. S. Cullick (1997). High resolution reservoir models integrating multiple-well production data. *SPE Annual Technical Conference*. San Antonio, Texas, October 5-8. SPE 38728.

10 Tables and figures

Reservoir characteristics; R							
Porosity; Φ		Permeability; K		Acoustic impedance; Z		Reflection coeff.; C	
σ_ϕ	0.015	$\sigma_{k,1}$	0.5	$r_{z,\text{top}}$	6473	σ_c	0.045
ν_ϕ	1.2	$\sigma_{k,2}$	0.62			ν_c	1.4
a	0.5430	ν_k	1.2				
b	$-4.5263 \cdot 10^{-5}$	t_z	5920				
		σ_{θ_1}	0.6				
		σ_{θ_2}	0.5				
		μ_{θ_1}	8.3				
		μ_{θ_2}	5.5				
		θ^t	$(8.5, 5.3)$				

Table 1: Model parameter values in prior model for reservoir variables.

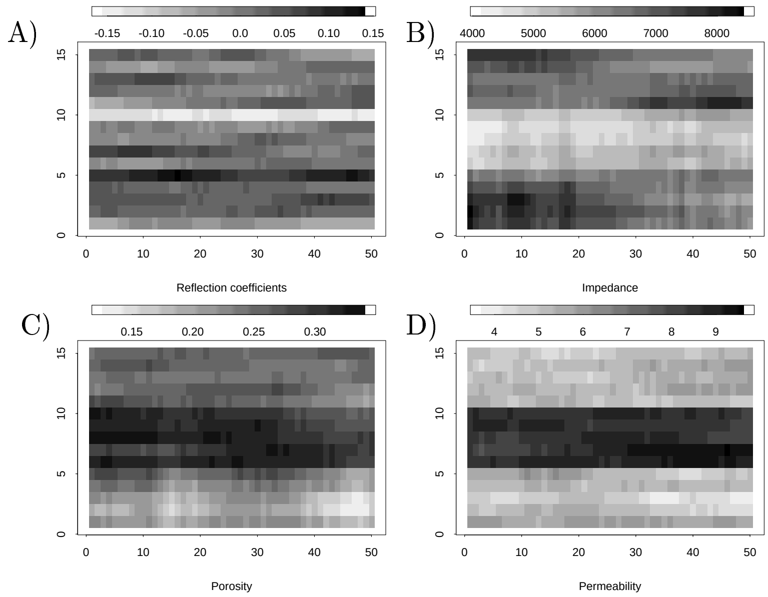

Figure 1: Cross section of reservoir variables in reference reservoir; A) reflection coefficients; B) acoustic impedance; C) porosity; D) absolute log-permeability

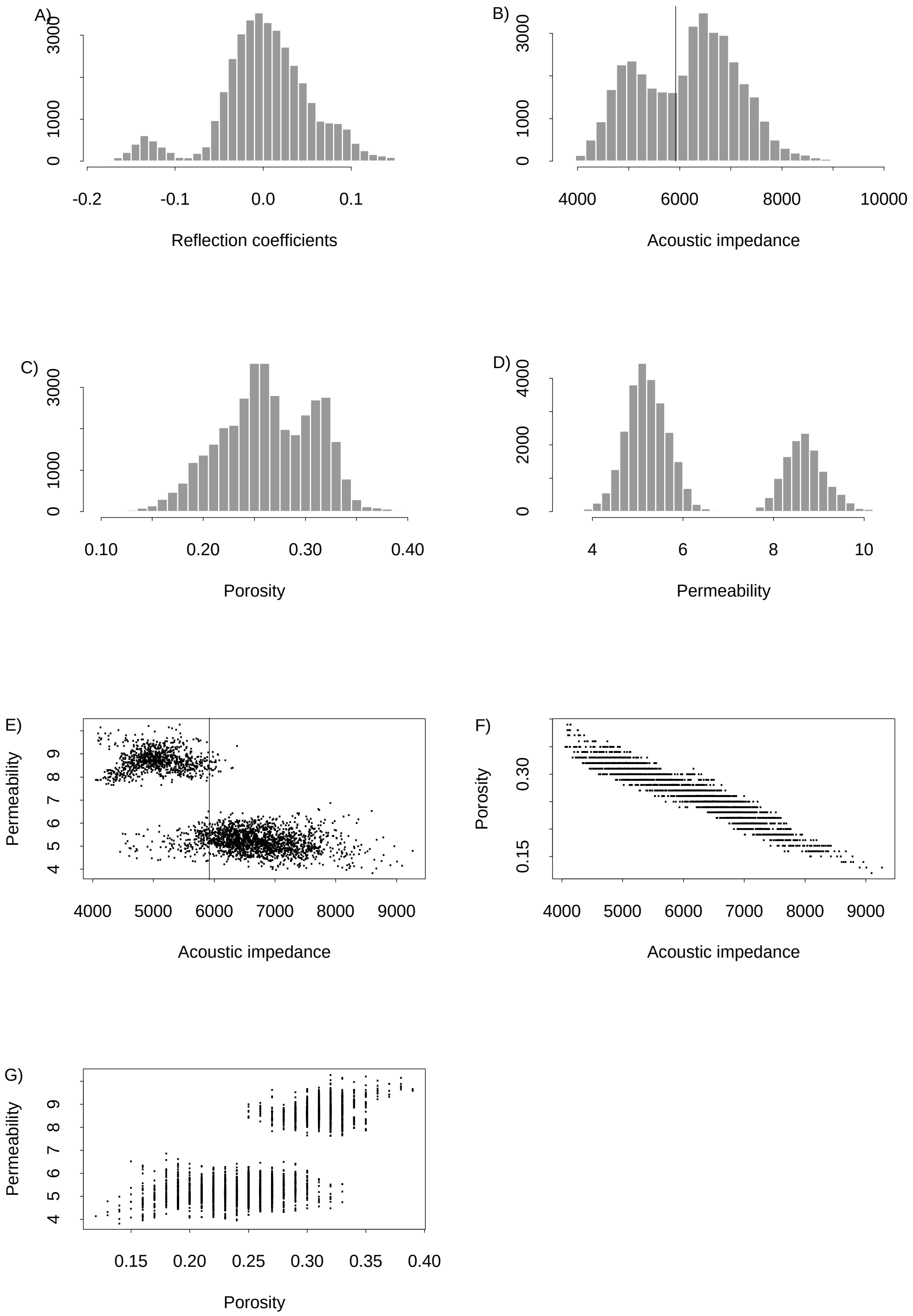

Figure 2: Statistics of reservoir variables of reference reservoir: A) reflection coefficients; B) acoustic impedance; C) porosity; D) log-permeability; E) acoustic impedance vs. porosity; F) acoustic impedance vs. log-permeability; G) porosity vs. log-permeability.

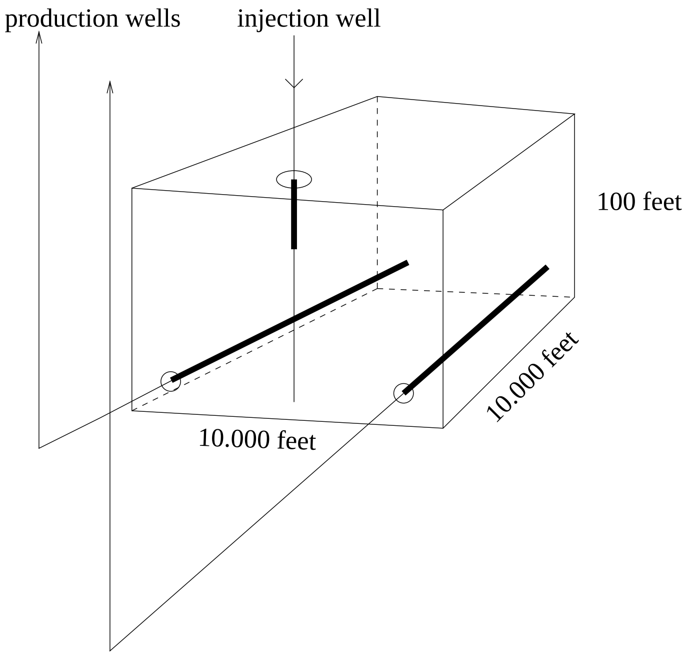

Figure 3: Reservoir outline and well configuration.

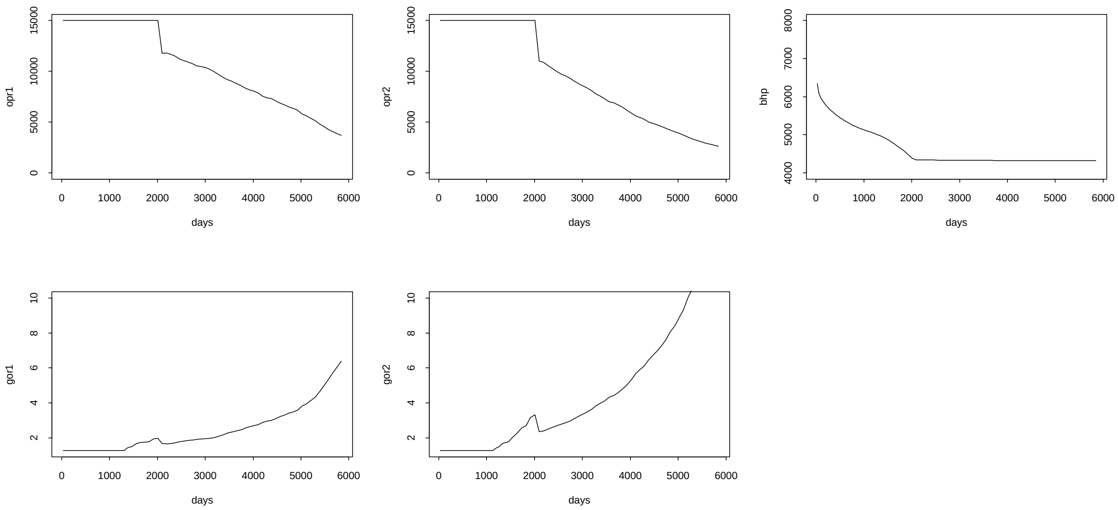

Figure 4: Production variables of reference reservoir.

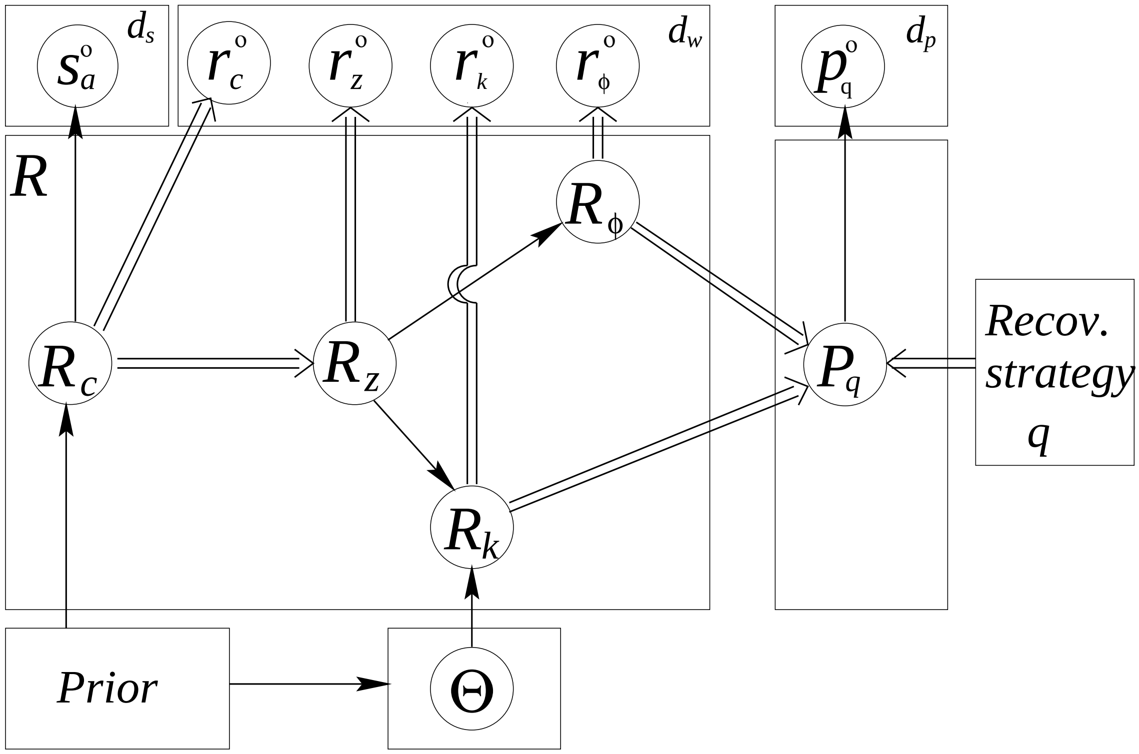

Figure 5: Graph of stochastic reservoir model.

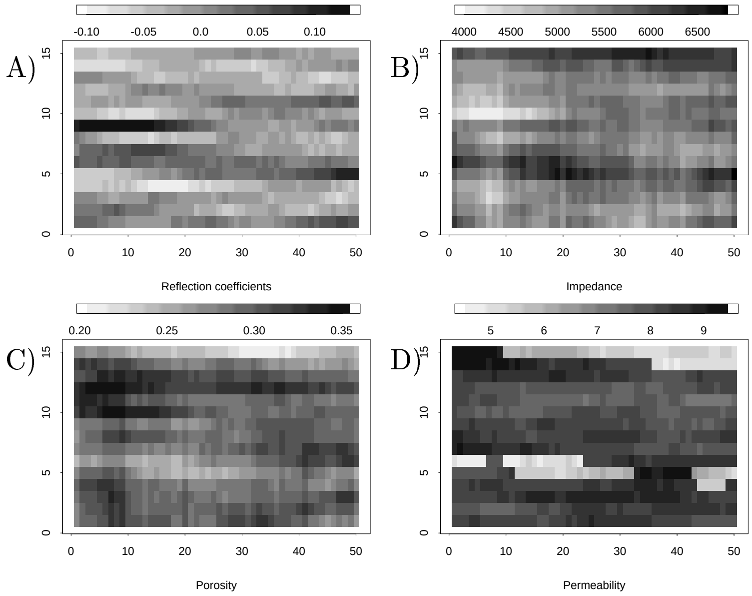

Figure 6: Cross section of reservoir variables from a representative sample from prior model; $f(r)$ A) reflection coefficients; B) acoustic impedance; C) porosity; D) absolute log-permeability.

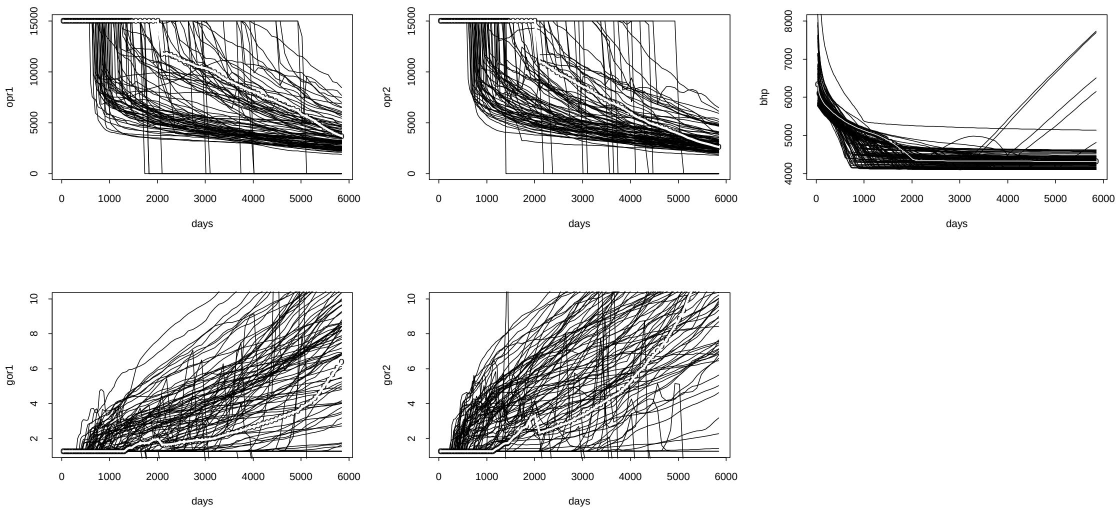

Figure 7: One hundred samples of production variables from prior model, given $\theta = \theta^t$, $f(p_q|\theta^t)$. Production variables of reference reservoir in white.

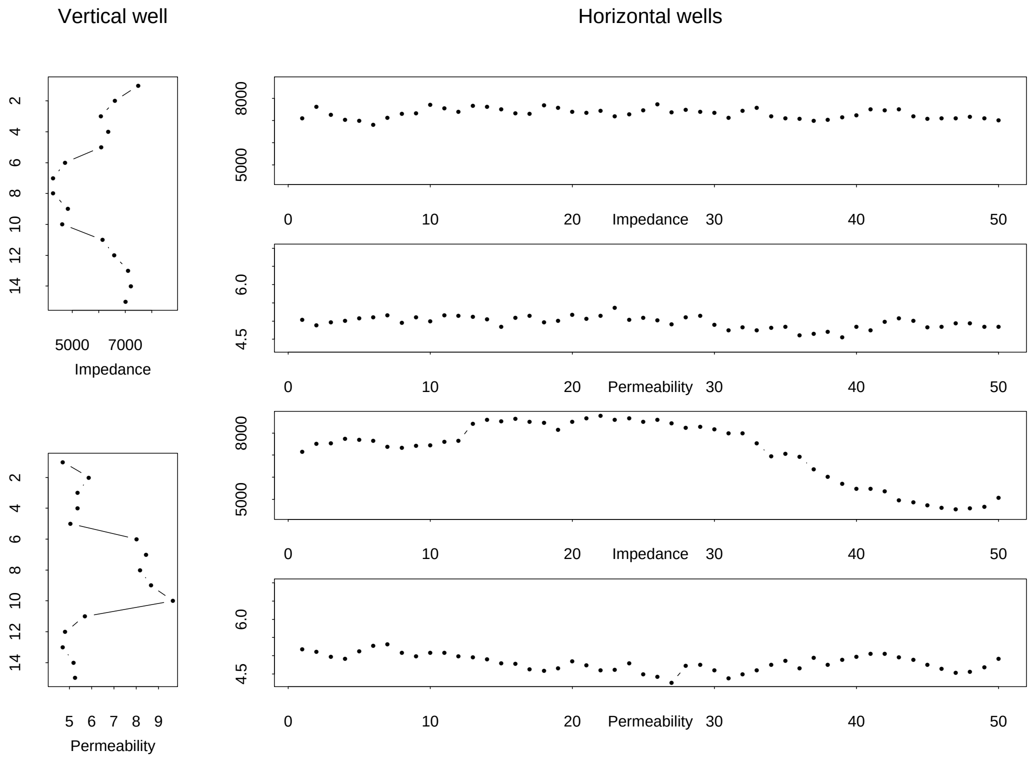

Figure 8: Example of well observations of log-permeability and acoustic impedance.

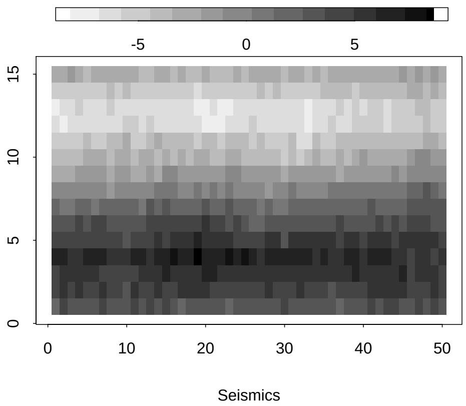

Figure 9: Cross section of seismic amplitude data.

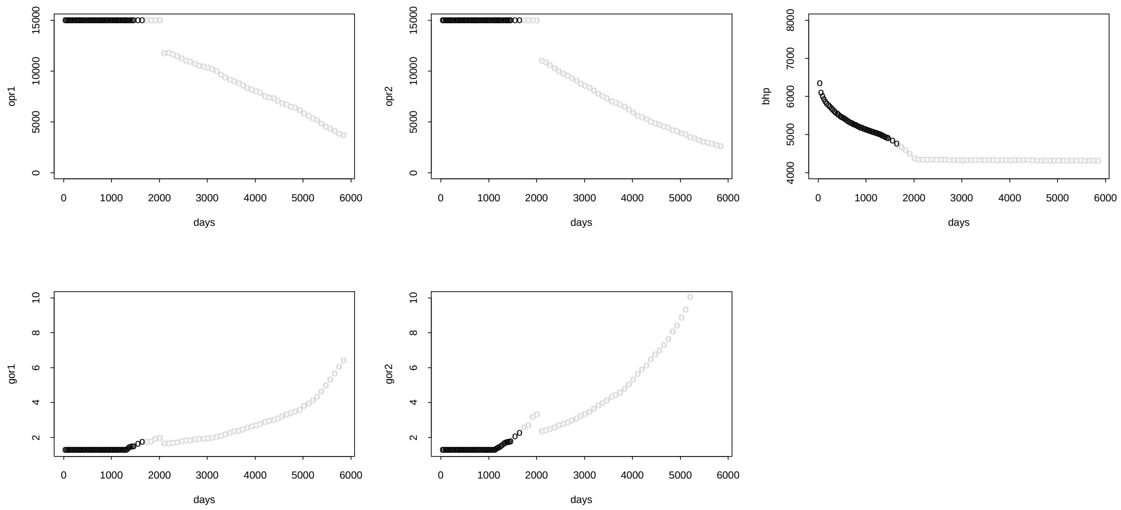

Figure 10: Production data for 4.5 years.

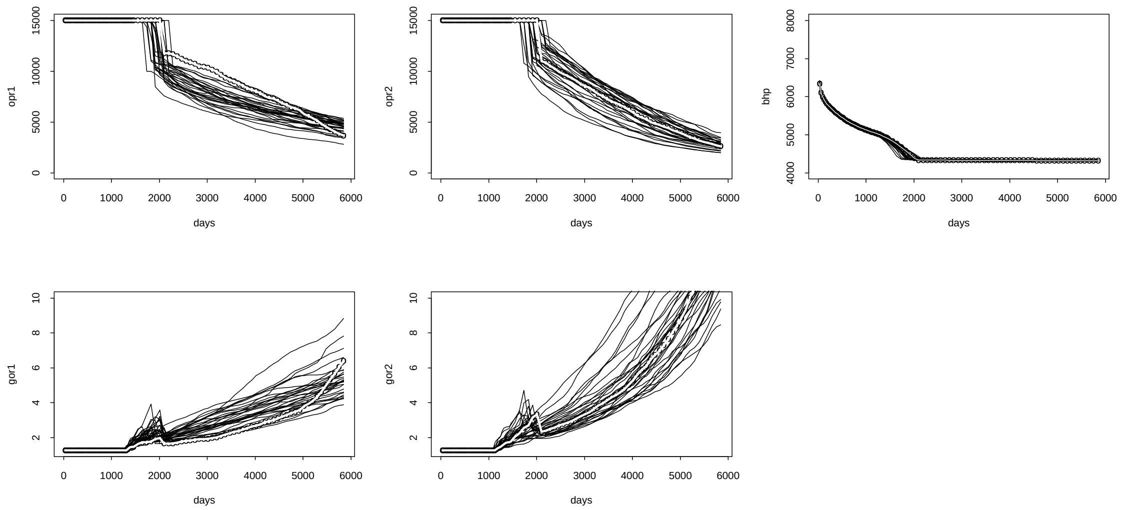

Figure 11: Thirty samples of production variables from posterior model $f(p_q|d_w, d_s, d_p)$. Production variables from reference reservoir in white.

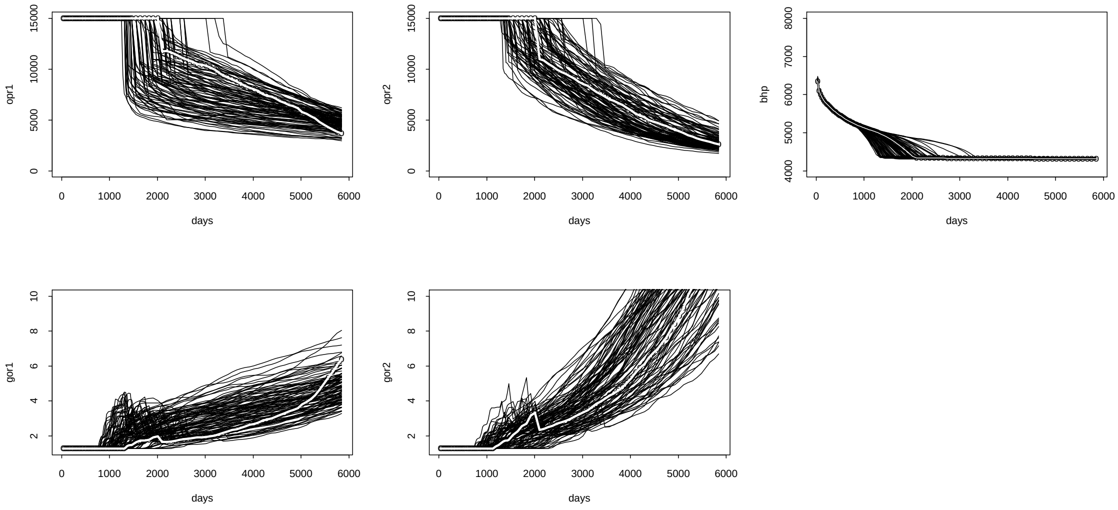

Figure 12: One hundred samples of production variables from pdf $f(p_q|d_w, \theta^t)$. Production variables from reference reservoir in white.

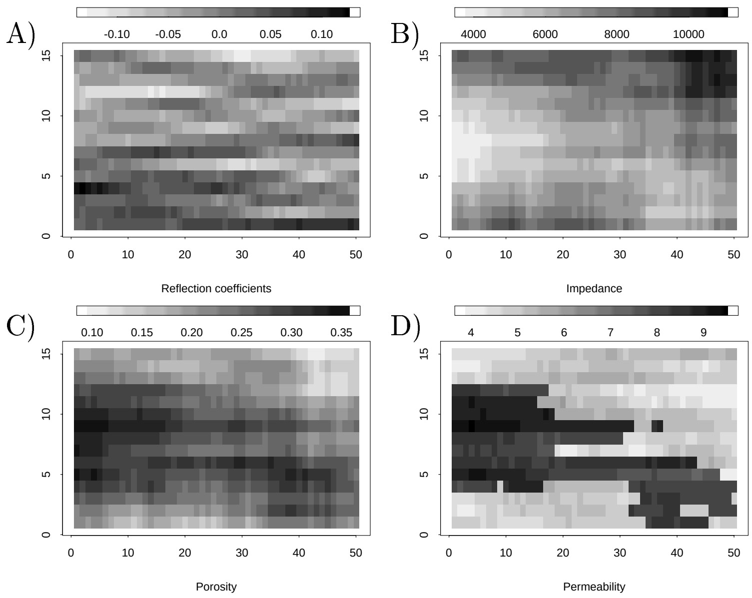

Figure 13: Cross section of reservoir variables from a representative sample from pdf $f(r|d_w, \theta^t)$.

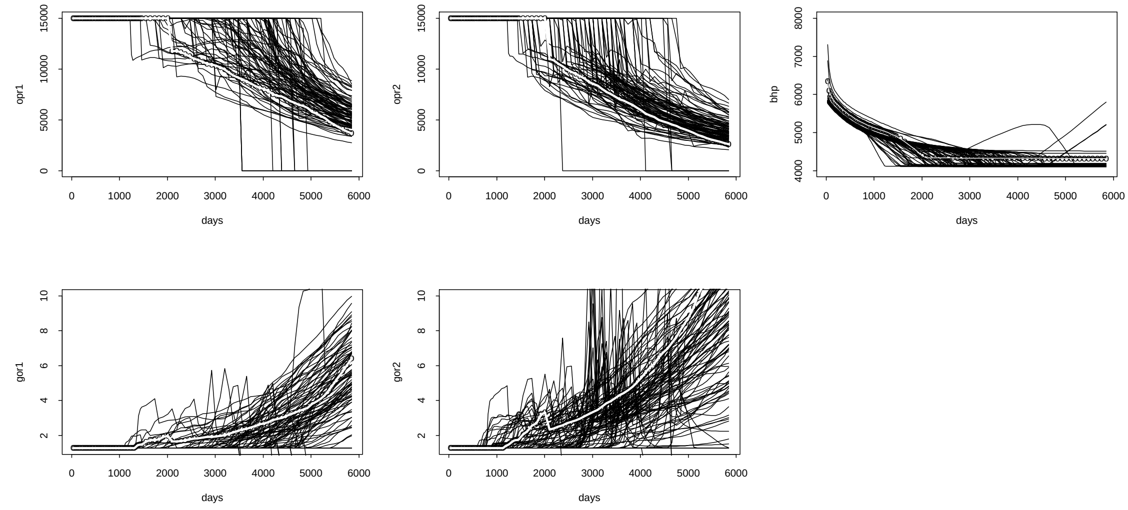

Figure 14: One hundred samples of production variables from pdf $f(p_q|d_s, \theta^t)$. Production variables from reference reservoir in white.

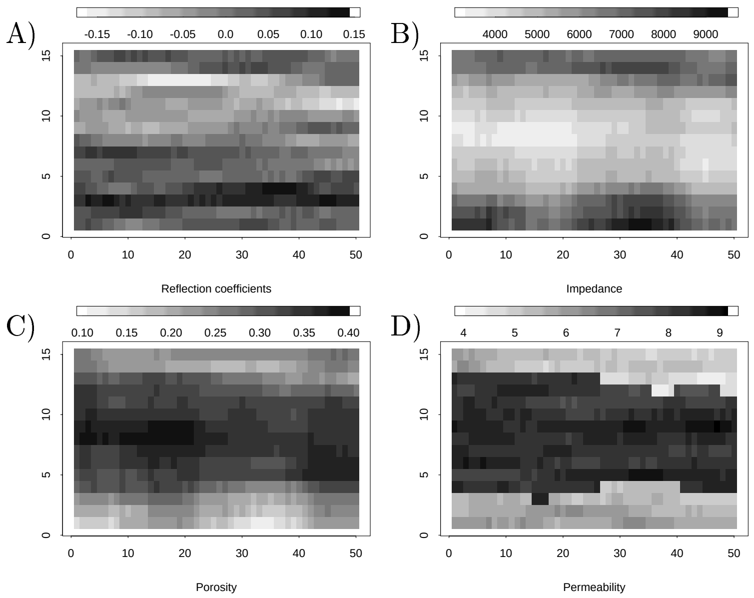

Figure 15: Cross section of reservoir variables from a representative sample from pdf $f(r|d_s, \theta^t)$.

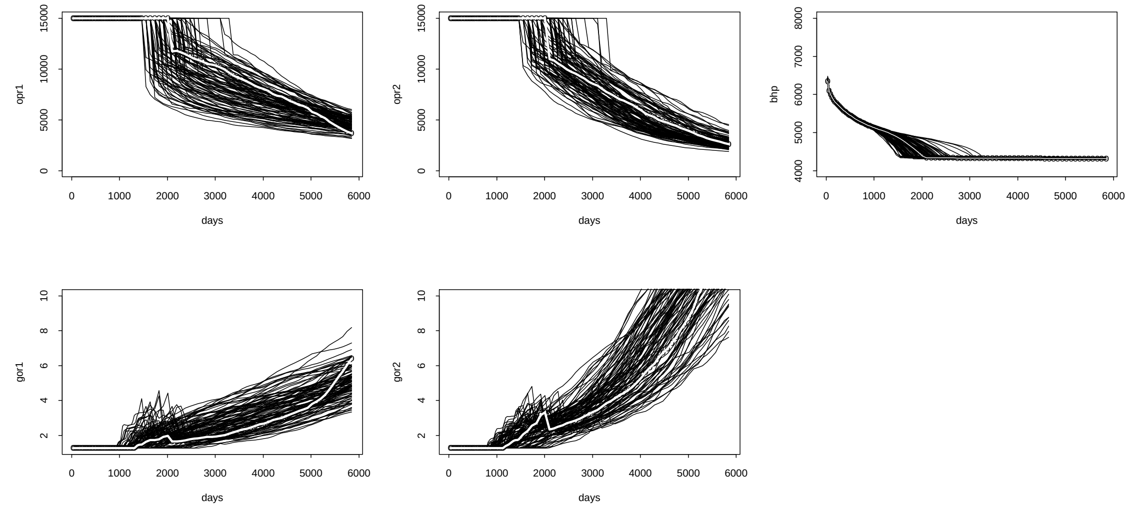

Figure 16: One hundred samples of production variables from pdf $f(p_q|d_w, d_s, \theta^t)$. Production variables from reference reservoir in white.

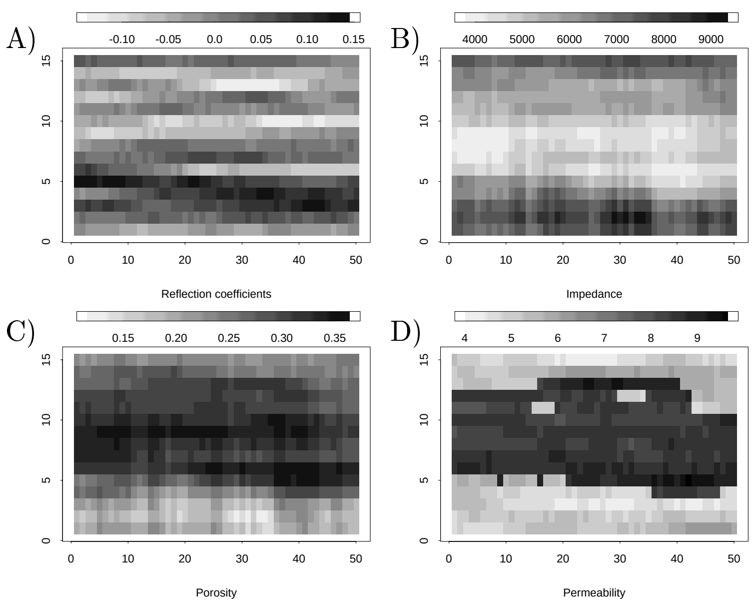

Figure 17: Cross section of reservoir variables from a representative sample from pdf $f(r|d_w, d_s, \theta^t)$.

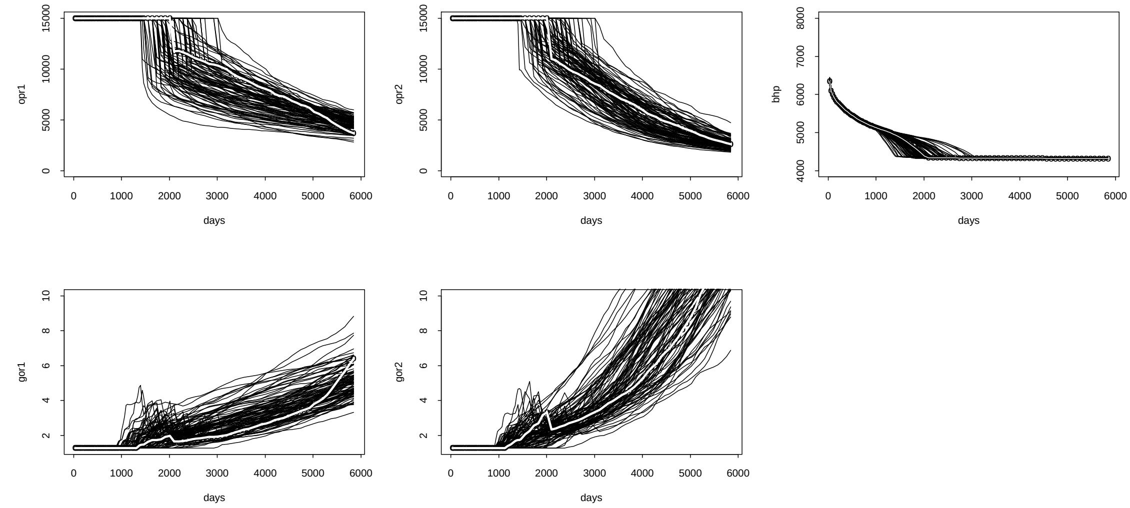

Figure 18: One hundred samples of production variables from pdf $f(p_q|d_w, d_s, d_p^*)$. Production variables from reference reservoir in white.

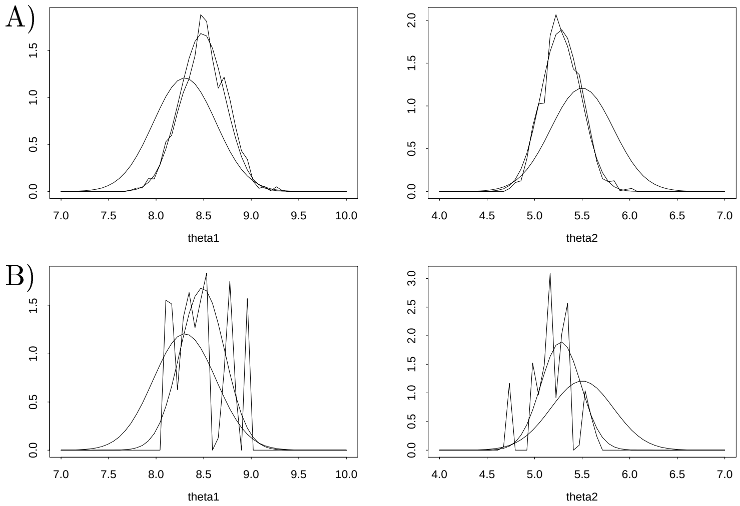

Figure 19: Level of log-permeability in the two facies, $\Theta = (\Theta_1, \Theta_2)$. Values in reference reservoir are $\theta^t = (8.5, 5.3)$. A) Displays of $f(\theta)$, $\hat{f}(\theta|d_w)$ and $\hat{f}(\theta|d_s, d_p^*)$. B) Displays of $f(\theta)$, $\hat{f}(\theta|d_w)$ and $\hat{f}(\theta|d_w, d_p)$.

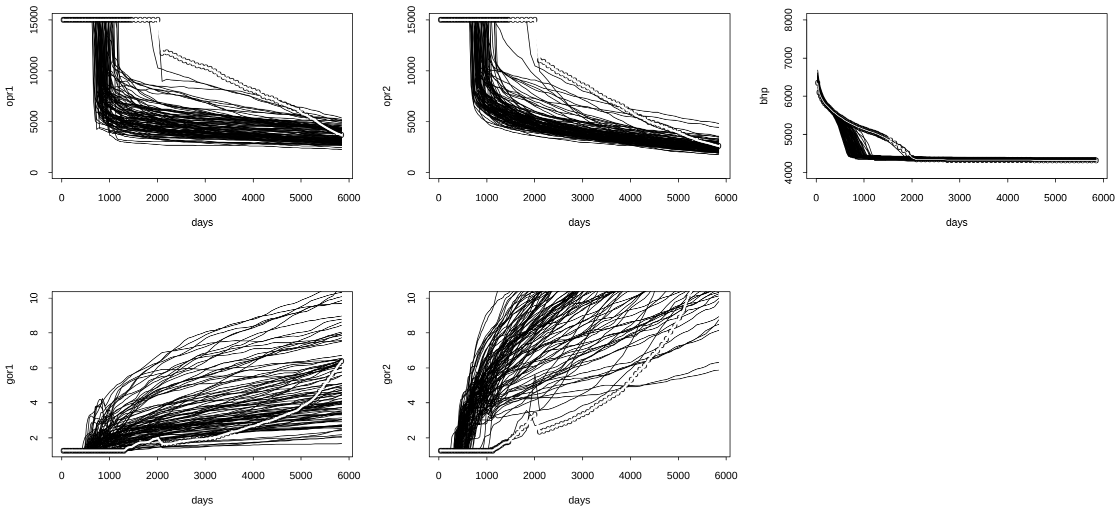

Figure 20: One hundred samples of production variables from pdf $f^u(p_q|d_w, \theta^t)$. Production variables from reference reservoir in white.

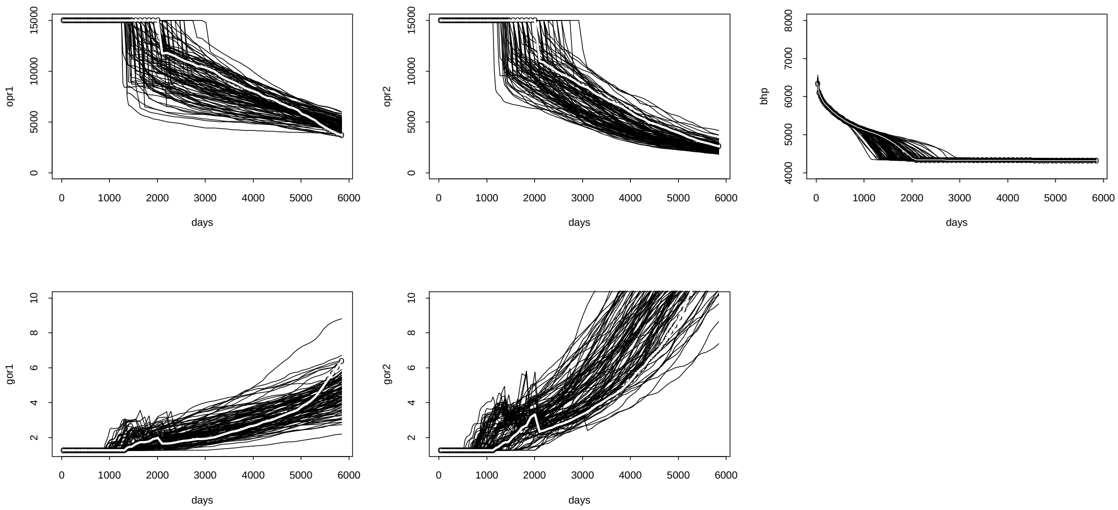

Figure 21: One hundred samples of production variables from pdf $f^u(p_q|d_w, d_s, \theta^t)$. Production variables from reference reservoir in white.